Global Biogeochemical Cycles

RESEARCH ARTICLE
10.1029/2018GB006030

Key Points:
- Permafrost thaw restructures subsurface flow paths and mobilizes dissolved organic matter transport within Arctic catchments
- Dissolved organic matter transport is appreciable at the permafrost-mineral interface, potentially reducing the terrestrial carbon sink
- The structural diversity of dissolved organic matter increases downslope and is greatest along the mineral-permafrost interface

Supporting Information:
- Supporting Information S1

Correspondence to:
L. M. Lynch,
lml262@cornell.edu

Citation:
Lynch, L. M., Machmuller, M. B., Boot, C. M., Covino, T. P., Rithner, C. D., Cotrufo, M. F., et al. (2019). Dissolved organic matter chemistry and transport along an Arctic tundra hillslope. *Global Biogeochemical Cycles*, *33*, 47–62. https://doi.org/10.1029/2018GB006030

Received 11 JUL 2018
Accepted 22 DEC 2018
Accepted article online 5 JAN 2019
Published online 23 JAN 2019

Dissolved Organic Matter Chemistry and Transport Along an Arctic Tundra Hillslope

Laurel M. Lynch[1,2], Megan B. Machmuller[2], Claudia M. Boot[2,3], Timothy P. Covino[2,4], Christopher D. Rithner[3], M. Francesca Cotrufo[2,5], David W. Hoyt[6], and Matthew D. Wallenstein[2,5]

[1]Section of Soil and Crop Sciences, College of Agriculture and Life Sciences, Cornell University, Ithaca, NY, USA, [2]Natural Resources Ecology Laboratory, Colorado State University, Fort Collins, CO, USA, [3]Central Instrument Facility CORE, Colorado State University, Fort Collins, CO, USA, [4]Ecosystem Science and Sustainability, Colorado State University, Fort Collins, CO, USA, [5]Department of Soil and Crop Sciences, Colorado State University, Fort Collins, CO, USA, [6]Environmental Molecular Sciences Laboratory, Pacific Northwest National Laboratory, Richland, WA, USA

Abstract Permafrost thaw is projected to restructure the connectivity of surface and subsurface flow paths, influencing export dynamics of dissolved organic matter (DOM) through Arctic watersheds. Resulting shifts in flow path exchange between both soil horizons (organic-mineral) and landscape positions (hillslope-riparian) could alter DOM mobility and molecular-level patterns in chemical composition. Using conservative tracers, we found relatively rapid lateral flows occurred across a headwater Arctic tundra hillslope, as well as along the mineral-permafrost interface. While pore waters collected from the organic horizon were associated with plant-derived molecules, those collected from permafrost-influenced mineral horizons had a microbial origin, as determined by fluorescence spectroscopy. Using high-resolution nuclear magnetic resonance spectroscopy, we found that riparian DOM had greater structural diversity than hillslope DOM, suggesting riparian soils could supply a diverse array of compounds to surface waters if terrestrial-aquatic connectivity increases with warming. In combination, these results suggest that integrating DOM mobilization with its chemical and spatial heterogeneity can help predict how permafrost loss will structure ecosystem metabolism and carbon-climate feedbacks in Arctic catchments with similar topographic features.

1. Introduction

Widespread permafrost thaw in high-latitude regions (Koven et al., 2009; Osterkamp & Romanovsky, 1999) could increase CO_2 release from soils to the atmosphere (Ernakovich et al., 2017; Natali et al., 2015; Schuur et al., 2009) and transform the hydrology of Arctic landscapes (Frey & McClelland, 2009; Rowland et al., 2010; White et al., 2007). While permafrost boundaries currently limit subsurface storage and control the routing of water, carbon (C), nutrients, and sediment across Arctic landscapes (Rowland et al., 2010), permafrost loss is projected to increase soil drainage and the connectivity of surface and subsurface flow paths (Walvoord & Kurylyk, 2016), with implications for catchment biogeochemistry (Harms & Jones, 2012; Vonk et al., 2015). Of particular interest is the fate of natural dissolved organic matter (DOM), which comprises the dominant and most mobile form of organic C in soil pore waters (Jansen et al., 2014; Kalbitz et al., 2003). The vast chemical diversity of DOM shapes microbial metabolism (Ernakovich et al., 2017; Mu et al., 2017), links terrestrial and aquatic environments (Battin, Luyssaert, et al., 2009; Kellerman et al., 2014), and influences landscape C balances (Mu et al., 2017). Understanding the chemical composition and mobilization potential of DOM is thus essential in determining the proportion of newly thawed soil C that is converted and released to the atmosphere as carbon dioxide (CO_2), incorporated into microbial biomass, or stabilized in the soil mineral matrix (Lynch et al., 2018). These dynamics will influence whether Arctic catchments, which currently contain nearly half of the world's soil organic C reservoirs, remain a globally relevant C sink.

Geophysical factors, such as soil moisture and hillslope angle, vary between landscape positions (Anderson et al., 2008; Kane et al., 1989; Klaus et al., 2013; Seibert et al., 2009; Weiler & McDonnell, 2006) and can modulate DOM residence time (Mu et al., 2017) and transformation potentials (Battin, Kaplan, et al., 2009) within a catchment. DOM mobilization through mineral soils is limited by low permeability and hydraulic conductivity (Cooper et al., 1993; Santeford, 1978). However, preferential flow mechanisms such as pipe networks (Carey & Woo, 2000), water tracks (Bowden et al., 2008), desiccation and contraction cracks (Lachenbruch, 1962; Woo, 2012), and macropore flow (Weiler & McDonnell, 2006) can increase DOM exchange between soil horizons and lead to the mass loading of DOM to recipient streams (Covino, 2017), particularly as permafrost thaws. While antecedent soil moisture conditions typically control when, and how extensively, preferential flow networks are activated (Weiler & McDonnell, 2006), water in saturated mineral soils can be discharged to porous organic horizons and released directly to streams (Hinton et al., 1994; Kirchner, 2003; Neilson et al., 2018; Zastruzny et al., 2017). Evidence that DOC exported from permafrost soils is susceptible to photodegradation and microbial consumption (Ward et al., 2017) suggests increasing connectivity of soil flow paths to sunlit waterways could amplify C-climate forcing (Cory et al., 2013). Although permafrost-influenced soils are an important source of chemical energy to stream ecosystems, we currently lack a quantitative understanding of how DOM is cycled through Arctic hillslope environments and how the residence time of water parcels in different landscape positions influences DOM reactivity.

The residence time of water as it is conveyed across the terrestrial landscape determines the extent to which microbial communities can metabolize and alter DOM chemistry before it enters surface waters (Battin, Kaplan, et al., 2009; Mu et al., 2017). Substrates with low physicochemical reactivity, including aromatic compounds and those with high C:N (Ward et al., 2017), may be utilized by microbial communities with low metabolic efficiency (Lynch et al., 2018), resulting in the release of CO_2 and CH_4 to the atmosphere (Cotrufo et al., 2013). In contrast, substrates with higher physicochemical reactivity, such as oxygen-bearing or low C:N compounds, may be preferentially incorporated into microbial biomass (Liang et al., 2017). As a result, the assimilated DOM pool may be homogenized to common microbial residues, including detrital proteins and lipids that promote organic matter (OM) aggregation and stabilization within the soil matrix (Koven et al., 2009). Increasing mineral exposure could sequester DOM at the permafrost thaw front (Schmidt et al., 2011), but mineral-sorbed DOM can be released back into soil pore water depending on redox conditions, bonding environment, and microbial metabolism (Herndon et al., 2017; Kaiser & Kalbitz, 2012; Keiluweit et al., 2017; Riseborough et al., 2008). Additionally, enhanced plant productivity and plant inputs in the Arctic (Natali et al., 2012; Rustad et al., 2001) could promote the destabilization of mineral-associated OM via "priming" mechanisms (Fontaine et al., 2007; Keiluweit et al., 2015; Wild et al., 2014), making DOM vulnerable to transport or microbial processing. Because pore water DOM has the potential to structure downslope metabolism and in-stream productivity, it is essential to understand how hillslope environments influence its transport and chemical transformation.

DOM is comprised of an amalgam of compounds including recently produced plant products, microbial metabolites, and OM fragments that have been extensively degraded and reprocessed (Liang et al., 2017). Consequently, DOM is one of the most heterogeneous natural mixtures and requires the adoption of higher-resolution chemical techniques to determine its structural composition (Kellerman et al., 2014; Woods, Simpson, Koerner, et al., 2011), transformation in pore water environments (Ward & Cory, 2015), and influence on terrestrial C balances (Roth et al., 2014). Here we use nuclear magnetic resonance (NMR) spectroscopy to improve our understanding of the fate of DOM as it is cycled in soil pore waters. Solution state ^{1}H-NMR offers a powerful, nontargeted approach that can quantitatively classify DOM structures and metabolites by taking advantage of the magnetic spin properties of certain nuclei, including ^{1}H and ^{13}C, among others (Simpson et al., 2012). In addition to providing complete, quantitative (via peak intensity), and structurally informative (via chemical shift) measures of DOM composition, distinct regions of NMR spectra correspond with characteristic molecular properties, shedding light on structural classes relevant to ecosystem metabolism.

In this study, we characterized DOM chemistry and transport from two landscape positions (hillslope and riparian) and two soil horizons (organic and mineral) within Imnavait Creek watershed in northern Alaska. Imnavait Creek is an acidic tussock-tundra site that has been extensively monitored (Cooper et al., 1993; Kane et al., 1989; McNamara et al., 2008) and is representative of large regions of low-gradient Arctic foothills that extend across much of the North Slope of Alaska (Walker & Walker, 1996). We applied a suite of complementary approaches, including solution-state ^{1}H-NMR and fluorescence spectroscopy, to characterize the chemical composition of pore water DOM. We assessed the mobilization and exchange potentials of DOM flowing through organic soils versus along the mineral-permafrost interface using

10.1029/2018GB006030

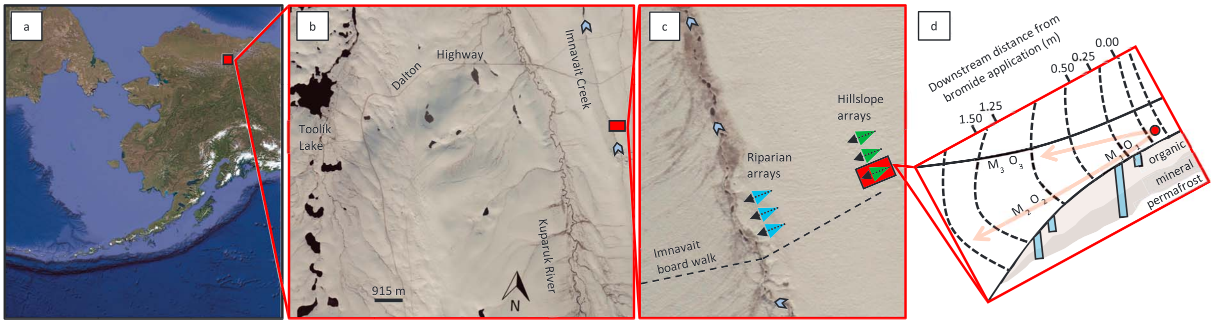

Figure 1. Study sites were located in northern Alaska (a) near Imnavait Creek (b, direction of stream flow shown by blue arrows). Three replicated lysimeter arrays were established in representative hillslope (green) and riparian (blue) landscape positions (c). At the top of each lysimeter array (d), we applied potassium bromide (red circle) to trace preferential flow paths and exchange potentials between organic and mineral soil horizons in hillslope and riparian positions (dotted contour lines are an idealized representation of slope angle and topography, the solid black line represents assumed downslope export of dissolved organic matter). At each array, lysimeters O_1, O_2, and O_3 were installed in the organic horizon, 12 cm below the soil surface, and lysimeters M_1, M_2, and M_3 were installed at the mineral-permafrost interface, approximately 50 cm below the soil surface (shown in blue). Lysimeters O_3 and M_3 (blue profiles not shown) were installed on a 45° angle from the site of bromide application (red arrow not drawn to scale) to estimate horizontal flows across the landscape.

bromide, a conservative salt tracer. We hypothesized that (1) DOM is rapidly exported through porous organic relative to mineral soils, with minimal exchange between the two horizons and (2) DOM composition converges from hillslope to riparian positions, as the abundance of homogeneous microbial metabolic products sequentially increases and DOM chemical diversity decreases. With this rationale, we evaluated two predictions: (1) organic and mineral soil horizons act as independent reactors, with distinct chemistries propagated downslope and (2) DOM diversity is significantly higher in hillslope than riparian landscape positions.

2. Materials and Methods

2.1. Field Site Characterization

Imnavait Creek is located in the northern foothills of the Brooks Range in Alaska, USA (68°37′N, 149°17′W; Figure 1). The small headwater basin is completely underlain by permafrost and drains approximately 2 km^2. Soil substrates were deposited during the Sagavanirktok glaciation, approximately 300,000 years ago, and classified as Histic Pergelic Cryaquepts (Walker & Walker, 1996). The porous organic horizon is comprised of live and dead roots, and the mineral horizon is made of silt overlying rocky glacial till and meltwater deposits capped by thick loess and solifluction lobes (Walker & Walker, 1996). The maximum thaw depth during sampling was 60 cm, which is within the 13-year average thaw depth of the Imnavait catchment (Kling, 2007).

Dry prostrate shrub and fruticose-lichen tundra dominate the hillcrest and shoulder of the Imnavait Creek catchment. Dominant hillslope vegetation consists of *Eriophorum vaginatum* (a tussock-forming sedge), *Betula nana* (a dwarf birch shrub), and mosses. Along the riparian corridor, the high abundance of *Sphagnum* mosses increases soil acidity and reduces active layer thickness (Walker & Walker, 1996). Imnavait Creek is a shallow beaded stream; ponded sections form at ice-wedge polygon intersections and are connected by short water courses (Walker & Walker, 1996). For the duration of this study—1 to 23 August 2016—cumulative precipitation was 58 mm, air temperature at 1 m ranged from −1.6 to 18 °C, average soil temperatures were 8 °C in the organic horizon (10 cm deep) and 4 °C in the mineral horizon (50 cm deep), and average in situ soil moistures were 32% (Toolik Lake EDC, Imnavait Creek SNOTEL Site # 968, 930-m elevation, North Slope County, 68°37′N by 149°18′W).

We measured soil bulk density at three locations in hillslope and riparian landscape positions. We carefully removed the aboveground litter layer and collected 10 × 10-cm^2 volumes of soil from the soil surface to the permafrost interface in 10-cm increments. We determined soil bulk density by dividing the dry mass by the volume of each sample. We used average organic and mineral bulk densities for subsequent statistical analyses.

2.2. Lysimeter Array

Two landscape positions (hillslope and riparian) were selected to assess flow pathways through organic and mineral soil horizons. On 2 August 2016, we installed three replicated arrays of clustered soil pore water samplers, hereafter referred to as lysimeters (1900L series from Soil Moisture Equipment Corp., Goleta, CA), at each landscape position, with six lysimeters per array (n = 36, Figure 1). Arrays were spaced 10 m apart from each other. Within each array we installed three lysimeters in the organic horizon (12 cm deep; depicted in Figure 1 as lysimeters O_1, O_2, and O_3), and three lysimeters at the mineral-permafrost interface (approximately 50 cm deep; depicted in Figure 1 as lysimeters M_1, M_2, and M_3). The first two sets of paired lysimeters were installed at a distance of 0.25 (O_1), 0.50 (M_1), 1.25 (O_2), and 1.50 (M_2) m directly downslope (180° angle) from the site of bromide application (see below) to assess the assumed primary flow paths. We installed a third pair of lysimeters 1.25 (O_3) and 1.50 (M_3) m down-valley (on a 45° angle) from the site of bromide application to capture potential lateral flow across the hillslope (Figure 1). We placed mineral horizon lysimeters 0.25 m downslope from the organic horizon lysimeters to minimize disturbance from installation.

We installed each lysimeter by digging a 10-cm diameter hole using a Dutch-style sandy soils auger, placing the lysimeter to the appropriate depth, and backfilling around the porous ceramic cup with silica flour to establish hydraulic contact between the soil matrix and sampling cup. We finished backfilling around the PVC tube with excavated soil. To collect pore water samples, we established a 65-centibar vacuum using a gauged vacuum hand pump (Soil Moisture Equipment Corp.) and sealed the lysimeter by folding over the Neoprene tubing and securing it with clamping rings. We extracted soil pore water from each lysimeter by unclamping the Neoprene tubing and connecting it to a 50-ml syringe or 1-L Erlenmeyer extraction kit. After recording the volume of pore water collected, samples were transferred to sterile 60-ml amber borosilicate bottles, and the vacuum was reestablished for the sampled lysimeter. Extraction lines and flasks were thoroughly rinsed six times with deionized water before subsequent sampling.

The location of each lysimeter was recorded using a Trimble GeoXT mapping grade receiver. Spatial characteristics were extracted from LiDAR data collected by Vierling et al. (2013). Elevation was calculated using the NAVD88 (vertical datum) and Geoid 12A. Terrain ruggedness was calculated as relative topographic position, where larger values correspond to greater surface roughness (Jenness, 2004). Relative topographic position was calculated as the difference between the maximum and minimum elevation at the location of each lysimeter, with a resolution of 25 cm. Aspect was measured relative to true north. All spatial characteristics are reported in Table S1 in the supporting information.

2.3. Pore Water Chemistries

We allowed the lysimeters to equilibrate for 1 week and purged them twice to minimize collection of samples influenced by soil disturbance. On 8 and 12 August 2016, we collected pore waters for detailed chemical analysis into sterile 60-ml amber borosilicate bottles, placed each bottle on ice in the field, froze them within 2 hr of collection and transported them to Colorado State University for analysis (described below). Dissolved organic carbon (DOC) and total dissolved nitrogen (TDN) concentrations were measured on a Shimadzu TOC-L (Shimadzu Scientific Instruments, Inc.) at the Fort Collins Biogeochemistry Laboratory, CO (U.S. Forest Service), with detection limits of 0.3 μM for DOC and 0.4 μM for TDN. Inorganic nitrogen (NO_3^- and NH_4^+) and phosphate (PO_4^{3-}) concentrations were measured on an Alpkem flow solution IV automated wet chemistry system (O.I. Analytical College Station, TX), with detection limits of 0.8 μM for NO_3^-, 2.8 μM for NH_4^+, and 0.5 μM for PO_4^{3-}.

Due to the remote location of our field site, we chose to freeze DOM samples, which is the preferred storage method for NMR analysis (Pautler et al., 2010; Rist et al., 2013; Woods, Simpson, Pautler, et al., 2011) but has been shown to affect optical fluorescence measurements (excitation-emission matrices [EEMS]). More specifically, freeze-thaw dynamics may alter fluorescent DOM composition and concentration (>10%) when sample aromaticity is high ($SUVA_{254}$ > 3.5 $L \cdot mg\text{-}C^{-1} \cdot m^{-1}$; Fellman, D'Amore, & Hood, 2008; Pokrovsky et al., 2018), although evidence is mixed (Coble et al., 2014; Otero et al., 2007; Spencer et al., 2010). We feel our EEMS results are robust because (1) $SUVA_{254}$ values (<3.0 $L \cdot mg\text{-}C^{-1} \cdot m^{-1}$) were below the threshold where significant alterations have previously been found (Fellman, D'Amore, & Hood, 2008), (2) DOM chemical composition and aromatic characteristics are similar to previously reported values for unfrozen

10.1029/2018GB006030

samples collected from the same sampling location (Imnavait watershed, Ward & Cory, 2015) and from other active layer soil horizons (low Arctic, Waldrop et al., 2010), (3) DOC concentrations are within range of groundwater samples collected the year prior from the same watershed (1,500–2,000 μM vs. 300–2,100 μM, respectively, Neilson et al., 2018) and DOC concentrations in unfrozen soil-water samples (Waldrop et al., 2010; Ward & Cory, 2015), (4) our NMR results support those found using EEMS, and (5) we observed no evidence of flocculation or production of brown particles in thawed samples, which is characteristic of abiotic particle formation and OM precipitation (Fellman, D'Amore, & Hood, 2008; Giesy & Briese, 1978).

2.4. Optical Fluorescence

We used fluorescence EEMS and specific ultraviolet absorbance to characterize the chromophoric and fluorescent properties of pore water samples using an Aqualog spectrofluorometer with a xenon excitation source (Horiba-Jobin Yvone Scientific Edison, NJ). We normalized samples to 5 mg-C/L, set the excitation and emission slits to a 3-nm band pass, and incrementally increased wavelength in 3-nm steps from 200 to 800 nm. A sealed cuvette of fluorescence-free DI water was used as a blank and analyzed between every 10 samples to correct for instrument drift. Following spectral analysis, each sample was corrected for inner-filter effects, Rayleigh scatter was masked using first and second grating orders, and the spectra were corrected by the sample blank to minimize the influence of water Raman peaks (Ward & Cory, 2015). We calculated DOC normalized specific ultraviolet absorbance at 254 nm ($SUVA_{254}$) by dividing the absorbance at 254 nm by the path length (m) and DOC concentration (mg-C/L). Resulting $SUVA_{254}$ values, reported as liters per milligram of carbon per meter, are used as an indicator of aromaticity (Weishaar et al., 2003). We quantified EEMS using the fluorescence regional integration approach as outlined by Chen et al. (2003) to identify five spectral regions (Matlab R2016b). EEMS regions I and II are related to simple aromatic proteins (similar to tyrosine and tryptophan), region III to fulvic-acid type material, region IV to soluble microbial byproduct-like material, and region V to humic acid-type organics (Chen et al., 2003). The fluorescence regional integration approach is well suited to capturing the underlying heterogeneity and compositional quality of aromatic DOM in soil pore waters because it quantifies regions of wavelength-dependent fluorescent intensities rather than selecting several data points per spectra (Chen et al., 2003).

2.5. NMR Spectroscopy

We lyophilized 60 ml of frozen water collected from each lysimeter using a FreeZone 6 Liter Console Freeze Dry System (Labconco Corp. Kansas City, MO). We relativized pore waters to the lowest C concentration (60.78 μM) and resuspended samples in a mixture of 10% deuterium (Cambridge Isotope Laboratories) and 90% HPLC-grade water (Sigma Aldrich). We transferred reconstituted samples to Wilmad 535-PP NMR tubes (Wilmad Glass, SP-Industries, Inc.) for high-precision analysis (McCay, 2009). All ^{1}H-NMR spectra were collected with a Varian Inova 500-MHz NMR spectrometer using a 1-D nuclear Overhauser effect spectroscopy (NOESY) presaturation experiment. Each experiment was performed with an actively shielded z gradient and a 3919 WATERGATE pulse sequence, which is favored in solution-state NMR for suppressing the water solvent peak at 4.7 ppm (Adams et al., 2013; McCay, 2009). We acquired spectra with 32 k time domain points and 1,024 scans at 298 K and reduced baseline distortions around the suppressed water peak using Crude and Whittaker smoothing. NMR regions were assigned the following chemical shifts based on their atomic composition and bonding properties: NMR region I (0.6–1.6 ppm) is characteristic of methyl, methylene, and methane bearing protons; region II (1.6–3.2 ppm) is characteristic of unsaturated functional groups, including ketone, benzylic, and allylic-bearing protons; region III (3.2–4.5 ppm) is characteristic of unsaturated, heteroatomic compounds, including O-bearing carbohydrates, ethers, and alcohols; region IV (6.5–8.5 ppm) is characteristic of conjugated, double bond functionalities, including aromatic, amide, and phenolic structures (Kalbitz et al., 2003; Simpson et al., 2007). We integrated the peaks beneath each bonding environment to calculate the relative contribution of each index in describing the structural composition of pore water DOM (Woods, Simpson, Koerner, et al., 2011, 2009). These assignments represent only the predominant species within each region; individual metabolites can exhibit proton resonance across multiple regional indices.

A subset of samples were diluted by 10% (v/v) with 5-mM DSS (2,2-dimethyl-2-silapentane-5-sulfonate-d6) as an internal standard at 0 ppm and analyzed at the Pacific Northwest National Laboratory using a Varian Direct Drive 600-MHz NMR spectrometer equipped with a 5-mm triple-resonance salt-tolerant cold probe. The 1-D spectra were processed using Chenomx NMR Suite 8.3 software, with peak quantification

10.1029/2018GB006030

assigned relative to the DSS internal standard. Candidate metabolites were identified by matching the chemical shift, intensity information, and J coupling to metabolite libraries available in the Chenomx library, and these 1-D ^{1}H spectra were collected as previously described (Dalcin Martins et al., 2017; Daly et al., 2016). For reference, the detection and concentration of annotated metabolites is provided for representative lysimeters in Table S2.We procured the InChI code for each annotated metabolite from PubChem and used ClassyFire to identify its chemical taxonomy (Feunang et al., 2016).

2.6. KBr Tracer Additions

To assess whether DOM mobilization differed between landscape position and soil horizon, we used potassium bromide (KBr) as a conservative hillslope tracer. We selected KBr because of low background concentrations at our field site, minimal adsorptive properties, and low toxicity (Davis et al., 1980). At each lysimeter array, we applied 1 L of 5-M KBr solution to the soil surface on 12 August 2016 (infiltration was instantaneous). We sampled lysimeters 5 and 8 hr after application (insufficient soil moisture at the hillslope position precluded extraction after 8 hr), and then once daily for 10 consecutive days, resulting in 14 samples per lysimeter at the riparian landscape position and 13 samples per lysimeter at the hillslope landscape position. We measured bromide concentrations on a Dionex ICS-3000 Ion Chromatograph at the Fort Collins Biogeochemistry Laboratory, CO (U.S. Forest Service), with a detection limit of 0.13 μM.

The changing bromide tracer concentration sampled through time is known as the breakthrough curve (BTC). We developed bromide tracer BTCs for each sampling lysimeter and used these data to calculate modal transport velocities. First, we calculated modal transit time as the time from tracer injection to the time to reach peak BTC concentration at each lysimeter. Next, we calculated modal transport velocities as the horizontal distance from the KBr application site to the sampling lysimeter (i.e., travel distance) divided by modal transit time. We focused on modal tracer velocities for two reasons: (1) The modal velocity is the most frequent velocity of the velocity distribution, and, 2) while BTCs at most sampling lysimeters reached peak BTC concentration and then began to decline, not all BTCs returned to background concentration. In cases where the BTCs did not return to background concentration, calculations of other components of the velocity distribution (e.g., median tracer velocities) would be incorrect. Conversely, calculation of modal velocity is only dependent on the time to reach peak BTC concentration and is not influenced by whether the BTC returned to background. We restricted our statistical analysis to estimate modal velocities for lysimeters that reached a clear peak BTC concentration ($n = 28$) during the sampling period (Figure S1). Lysimeters that did not reach peak BTC after 10 days were primarily installed in the mineral horizon down-valley (at a 45° angle) from the site of bromide application (M_3 lysimeters as depicted in Figure 1), where slower dispersive forces seemingly dominate DOM transport.

2.7. Statistical Analyses

We used linear mixed-effects models to test the effect of landscape position (hillslope vs. riparian) and soil horizon (organic vs. mineral) on DOM properties and modal tracer velocities using the lme4 package (Bates et al., 2016) in R version 3.3.1. Landscape position, soil horizon, and their interaction were included as categorical fixed effects, and the blocked array design was included as a categorical random effect. Data were log transformed when necessary to meet assumptions of normality, evaluated with Shapiro-Wilk tests. Model residuals were inspected for constant and homogenous variance using Q-Q and residual versus fitted plots and formally tested with normal and studentized Breusch-Pagan tests and nonconstant variance scores. We summarized our model output using the lsmeans package (Table 1), which provides pairwise comparisons among least squares means and Tukey's Honestly Significant Difference adjusted p values (Lenth, 2016).

We identified relationships between our dependent variable of interest (modal tracer velocity, pore water chemistry, regional EEMS indices, and NMR bonding environments) and potential predictor spatial variables using multiple linear regression analysis. We identified highly correlated variables using Pearson correlation plots (Figure S2) and calculated variation inflation factors for each parameter in the model using the *vif* function in the R *car* package (Fox & Monette, 1992). We assigned a variation inflation factor cutoff value of 2 (Zuur et al., 2010) and sequentially removed variables until only independent predictor variables remained (Duffy et al., 2016). Potential variables for the initial regression analysis included surface roughness, slope angle, aspect, distance from Imnavait creek, and soil bulk density. Stepwise multiple linear

10.1029/2018GB006030

Table 1
Biogeochemical Characteristics of Soil Pore Water Samples Collected From Hillslope or Riparian Landscape Positions

Landscape position	Soil horizon	Modal velocity (m/hr)	DOC (μM)	TDN (μM)	NH_4 (μM)	PO_4^{3-} (μM)	EEMS I	EEMS II	EEMS III	EEMS IV	EEMS V	$SUVA_{254}$	NMR I	NMR II	NMR III	NMR IV
Hillslope	Organic	0.017	1916.31	57.97	3.99	1.42	16.27	36.76	23.00	16.11	7.86	2.61	13.15	16.24	8.07	20.41
		(0.010)	(137.21)	(7.39)	(1.54)	(0.05)	(2.31)	(0.87)	(1.26)	(0.25)	(0.53)	(0.11)	(0.25)	(0.13)	(0.13)	(0.40)
	Mineral	0.010	1759.45	51.79	2.53	1.24	15.91	40.70	20.11	16.77	6.52	2.96	12.32	16.23	8.41	19.32
		(0.003)	(118.98)	(4.76)	(0.42)	(0.03)	(1.03)	(0.64)	(0.94)	(0.15)	(0.36)	(0.06)	(0.28)	(0.16)	(0.28)	(0.37)
Riparian	Organic	0.029	1521.42	56.16	3.50	1.28	14.88	36.36	24.57	15.99	8.20	2.65	13.84	15.27	7.58	21.50
		(0.018)	(109.62)	(8.23)	(0.78)	(0.05)	(1.73)	(1.01)	(0.72)	(0.21)	(0.24)	(0.06)	(0.37)	(0.62)	(0.08)	(0.50)
	Mineral	0.022	1757.18	91.15	9.19	1.13	13.44	40.96	21.43	17.23	6.94	2.83	12.68	16.30	7.95	20.04
		(0.012)	(201.29)	(18.05)	(2.56)	(0.03)	(0.87)	(0.63)	(0.44)	(0.24)	(0.14)	(0.08)	(0.43)	(0.19)	(0.26)	(0.56)
Source of variance																
L		ns	ns	ns	ns	***	ns	ns	ns	ns	ns	ns	ns	ns	ns	*
H		ns	ns	ns	**	***	ns	***	**	***	***	**	**	ns	ns	**
L*H		ns	ns	* *	***	ns	ns	ns	ns	ns	ns	**	ns	*	*	ns

Note. At each landscape position, samples were collected from either the organic horizon or along the mineral-permafrost interface. Values are the average followed by the standard error in parentheses below, for modal velocity (including only lysimeters with clear bromide tracer breakthrough curve peaks). DOC = dissolved organic carbon; TDN = total dissolved nitrogen; NH_4 = ammonium; PO_4^{3-} = phosphate; regions I–V are related to EEMS indices described in Figure 2; $SUVA_{254}$ = DOC normalized specific UV absorbance at 254 nm, reported in liters per milligram of carbon per meter (aromaticity index); NMR I (0.6–1.6 ppm: methyl, methylene, and methane bearing protons); Region II (1.6–3.2 ppm: unsaturated functional groups); Region III (3.2–4.5 ppm: unsaturated, heteroatomic compounds); Region IV (6.5–8.5 ppm: conjugated, double bond functionalities). The level of significance from the two-way analysis of variance model including landscape position (L), soil horizon (H), and their interaction (L*H) are reported as *$p < 0.05$, **$p < 0.01$, ***$p < 0.001$, or nonsignificant (ns). EEMS = excitation-emission matrices; NMR = nuclear magnetic resonance.

regressions were conducted following Sutfin and Wohl (2017) using the *step* function in the R *stats* package with Akaike information criterion as the model selection criterion. We normalized TDN, PO_4^{3-}, EEMS regions IV and V, and modal velocity using boxcox power transformations in the R *MASS* package and verified assumptions of normality and constant and homogenous variance as above (regression output and λ values are reported in Table S3). To test for an association between fluorescence composition and spatial or chemical drivers, we used constrained analysis of principal components (capscale), an ordination method available in the R *vegan* package (Oksanen et al., 2007). We computed Bray-Curtis dissimilarities from fluorescence indices and fit 15 potential drivers to the ordination (Figure S3), before limiting drivers to include only those variables contributing to sample separation in ordination space (defined as eigenvalues >0.5); p values were calculated over 2,000 permutations.

We used MetaboAnalyst 3.0 (Xia & Wishart, 2016) to process and analyze NMR metabolites (following removal of the solvent peak at a shift of 4.5–5.0 ppm). We sum-normalized and z-transformed variables and removed noninformative spectral regions using interquartile range filtering, a recommended data pretreatment step for untargeted metabolomics data sets (Hackstadt & Hess, 2009). We used partial least squares-discriminant analysis, a method commonly applied to chemometric data sets (Grootveld, 2014), to determine whether samples clustered by categorical factors (landscape position or soil horizon) using the *plsr* function in the R *pls* package (Wehrens & Mevik, 2007). We explored relationships between the distribution and intensity of the metabolites and classification system (landscape position or soil horizon) using random forest classification and B/W permutation tests and assessed the performance of each generated model with tenfold cross-validation methods. For each model, we generated 2,000 permutations to test whether our hypothetical classification systems were significantly better than those arising through random chance (Grootveld, 2014).

3. Results

3.1. Influence of Landscape Position and Soil Horizon on Pore Water Chemistry

Contrary to our expectations, variation in DOC concentrations was not explained by landscape position or soil horizon (Figure S4 and Table 1). We observed significant interactions between landscape position and soil horizon for TDN and NH_4^+ pools (Table 1). TDN concentrations were 1.6 times higher in pore waters collected at the mineral-permafrost interface than those collected from the organic horizon of the riparian corridor ($F_{1,28} = 0.58$, $p < 0.01$, Figure S4) and NH_4^+ concentrations were twice as high in riparian mineral soils than all others ($F_{1,28} = 1.69$, $p < 0.001$). Pore water nitrate concentrations were below detection limit (<0.8 μM). We observed main effects of landscape position and soil horizon (no interaction) on pore water PO_4^{3-} concentrations, which were 14% higher in overlying organic than mineral soils ($F_{1,32} = 21.26$, $p < 0.001$) and 10% higher on the hillslope than along the riparian corridor ($F_{1,32} = 16.07$, $p < 0.001$, Figure S4).

Optical fluorescence characteristics, which characterize the chromophoric fraction of DOM, were not influenced by landscape position but differed significantly between soil horizons (Table 1). The relative percent intensities for EEMS regions II and IV, related to simple aromatics and soluble microbial-type proteins, were 12% and 6% higher in pore waters collected at the permafrost-mineral interface than those collected in the upper organic horizon ($F_{1,28} = 37.25$, $p < 0.001$ and $F_{1,28} = 21.12$, $p < 0.001$, respectively). In contrast, regions III and V, related to plant-derived compounds, exhibited 25% and 8% higher relative fluorescence intensities in the organic than the mineral horizon ($F_{1,28} = 15.10$, $p < 0.001$ and $F_{1,32} = 18.94$, $p < 0.001$, respectively). Regressing region IV against region V revealed a strongly negative relationship (adjusted $r^2 = 0.54$), suggesting microbe-derived products are enriched at depth (Figure S5). We also observed a significant interaction between landscape position and soil horizon on DOM aromaticity, with significantly higher $SUVA_{254}$ values in hillslope mineral than hillslope organic soil horizons ($F_{1,28} = 0.14$, $p < 0.01$). Using constrained analysis of principal components, we identified five drivers associated with fluorescence composition that separated pore waters collected from the mineral and organic horizon (Figure 2). Within ordination space, principal coordinate 1 explained 32% of the variation across the data set and principal coordinate 2 explained an additional 8%. Pore waters with aromatic contributions from EEMS regions II and IV were associated with greater bulk densities ($p < 0.001$) and structural features characteristic of O-bearing carbohydrates, ethers, and alcohols functionalities. In contrast, EEMS regions III and V, indicative of plant-derived compounds,

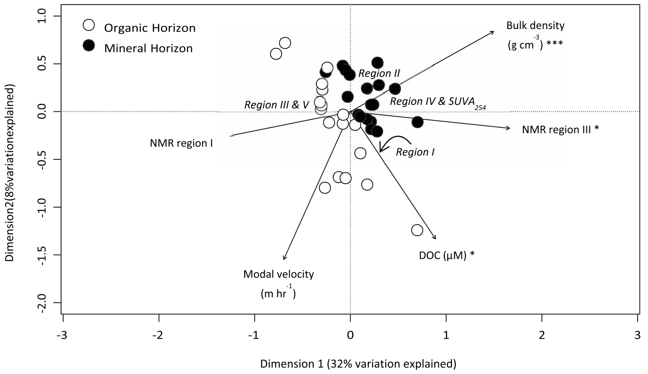

Figure 2. Multivariate analysis of fluorescence data and drivers using constrained analysis of principal components (capscale). Ordinations are based on Bray-Curtis dissimilarity. Pore water samples were collected from the organic (open symbol) or mineral (closed symbol) soil horizons. Spatial and pore water variables with eigenvalues >0.5 are fit to the ordination. Variables with a significance level of <0.05 (*), <0.01 (**), and <0.001 (***) were identified using analysis of variance with 2,000 permutations.

were associated with preferential, downslope flows through organic soil horizons, and greater structural diversity within lower chemical shift regions.

3.2. Metabolite Characterization (NMR Analysis)

We observed significant structural variability in pore water chemistries collected from hillslope and riparian landscapes as well as from organic and mineral soil horizons (Figures 3 and S6). Results were consistent across multiple spectral integration approaches (not integrated, integrated by regional index, or integrated by parts per million shift, data not shown). Together, the first two partial least squares-discriminant analysis components explained 47% of the variance, with maximal classification performance achieved with five components ($r^2 = 0.87$; CV accuracy = 0.61). The overall random forest out-of-bag error was 0.56, with the best classification achieved for riparian organic pore waters (0.33). Classification error was highest (0.88) for hillslope organic soils, which featured a core set of metabolites common across the landscape.

NMR regions I and IV, indicative of aliphatic chains and conjugated aromatic compounds, were 8% and 6% higher in organic soil horizons than at the mineral-permafrost interface (Table 1, $p < 0.01$). We observed a significant interaction between landscape position and soil horizon on proton resonances within region II, which were enriched along the permafrost interface of the riparian landscape position and are associated with highly processed, refractory compounds (Hertkorn et al., 2006) as well as allylic and ketone-bearing groups. Proton resonance within region III, associated with carbohydrate and other heteroatom-bearing compounds, accounted for only 8% of all spectral features and were marginally more abundant at the hillslope position (Table 1, $p = 0.08$). Formate, a derivative of C3 plants, and acetate were the most abundant metabolites, with higher concentrations in hillslope soils. Fermentation byproducts, including methanol, isopropanol, and lactate were also present and enriched in mineral soils. Several short-chain fatty acids, including suberate, butyrate, and isovalerate were present in relatively low concentrations (<22 μM) across landscape positions and indicative of microbial metabolism (Table S4).

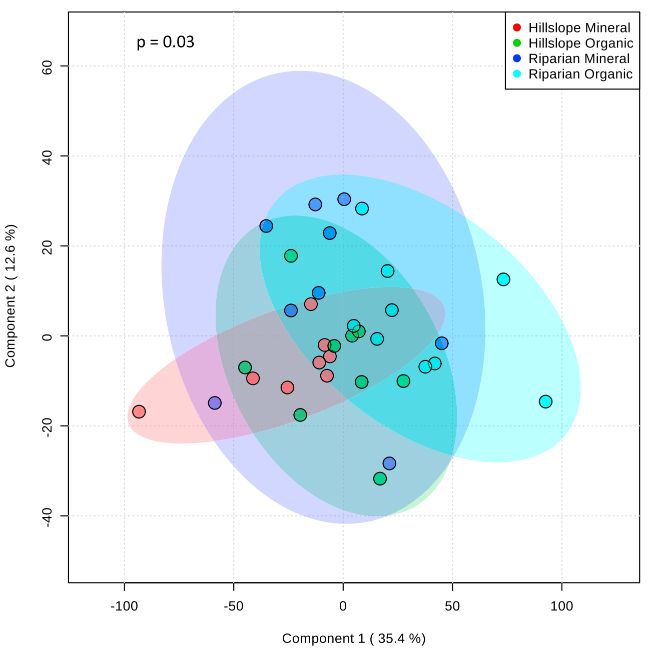

Figure 3. Partial least squares-discriminant analysis plot of dissolved organic matter from [1]H-NMR analysis clustered by landscape position and soil horizon. Each circle represents a sample and shaded ellipses represent 95% confidence intervals for each a priori cluster. Ellipse overlap signifies no significant difference between clusters. Two thousand permutations were generated to test whether our classification systems (landscape position and soil horizon) were significantly ($p < 0.05$) better than those arising through random chance.

3.3. Environmental Drivers of DOM Mobilization

During our observation period, bromide concentrations did not peak at five lysimeters installed in the mineral horizon down-valley (at a 45° angle) from the site of bromide injection, suggesting dispersive flow is slower than down-gradient flow along the hillslope. After restricting our analysis to include only lysimeters with clear bromide tracer BTC peaks, we found that modal velocities did not differ significantly across landscape positions or between soil horizons (Figure 4). For reference, it would take approximately 6 days for DOM to travel 1 m directly downslope. Soil bulk density explained 18% of the variability in modal velocities ($p < 0.01$) and reduced the best-fit Akaike information criterion model scores by 4.6 relative to the null model (Table S2).

4. Discussion

Rapid warming in high-latitude regions is expected to thaw permafrost and mobilize pore water DOM through deep flow paths. The results of this study advance our understanding of how the transport and transformation of DOM within a headwater tundra catchment influences its fate. Combining hillslope connectivity with DOM chemistry provides unique insight into pore water cycling, which is critical to understanding the

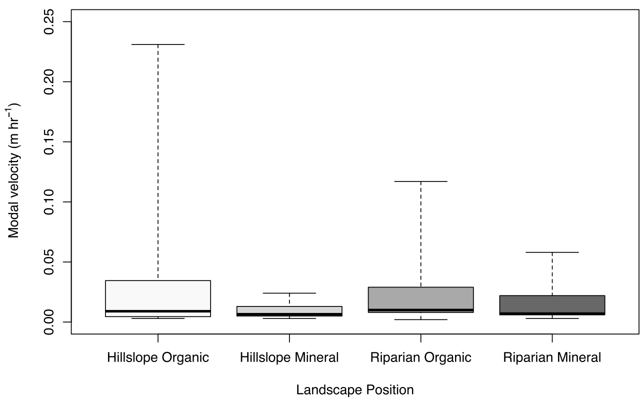

Figure 4. Boxplot panels representing the modal velocity of bromide intercepted from lysimeters installed in the hillslope or riparian landscape position and from organic or mineral soil horizons (excluding lysimeters that did not reach peak breakthrough curve bromide concentrations during the 10-day sampling period). Modal velocities were not significantly different between soil horizons ($p = 0.20$) or landscape position ($p = 0.90$). Each box spans the interquartile range and whiskers extend to the minimum and maximum of the distribution ($n = 6$).

interactive metabolism of terrestrial and aquatic environments (Figure 5). We found that compounds mobilized through the porous organic horizon were associated with plant-derived molecules, while those flowing through mineral soils had a microbial footprint. Landscape position also influenced the structural diversity of DOM, which increased during downslope transport from hillslope to riparian soils. While the chemical composition of DOM varied across the hillslope, the potential for relatively rapid subsurface flow and along the mineral-permafrost interface suggests that DOM mobilization may be a critical mechanism of C loss from Arctic catchments with similar topographies.

The release of pore water DOM across the terrestrial-aquatic interface is related to the connectivity of hillslope flow paths (Ameli et al., 2016; Tetzlaff et al., 2015) and seasonal variability in subsurface storage capacities (Carey & Quinton, 2005; Koch et al., 2013). Within similar low-gradient Arctic watersheds, permafrost losses are expected to deepen hydrologic flow paths and increase groundwater flows (Blaen et al., 2014; Vonk et al., 2015; Walvoord & Kurylyk, 2016; White et al., 2007). While the vertical decrease in soil bulk density was a significant predictor of modal tracer velocities, our results suggest deepening downslope flow paths will not substantially retard DOM delivery to surface waters. Relatively fast DOM mobilization through mineral soils has been observed within thin saturated layers that can develop at the base of the active layer as a result of infiltration, and via fill-spill mechanisms that are controlled by permafrost microtopography (Zastruzny et al., 2017). Similar work by Neilson et al. (2018) suggests substantial surface-subsurface (up to 30 cm deep) exchanges of water occur during downslope transport and are driven by local topography and vertical decreases in subsurface permeability. These findings help explain consistent DOC concentrations across landscape positions and soil horizons, which correspond to low variability in DOC concentrations delivered to Imnavait Creek across a range of hydrologic states and flow path depths (Neilson et al., 2018). However, we observed significant differences in the molecular composition of DOM between soil horizons, suggesting that pore waters are not fully mixed during vertical exchange. These findings are in agreement with work conducted in water tracks—zero-order hillslope channels with perennial subsurface flows—that balance the seasonal transport and reactivity of DOM delivered to surface waters as a result of thaw depth and antecedent moisture conditions. Lysimeters installed in the mineral horizon and down-valley (at a 45° angle) from the site of tracer injection did not reach peak bromide concentrations after 10 days, which suggests permafrost microtopography complicates flow networks and may extend

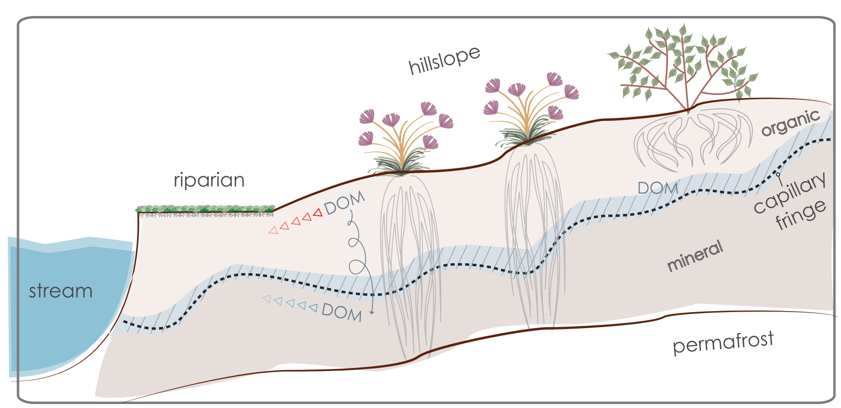

Figure 5. Conceptual model depicting the downslope transport and transformation of dissolved organic matter (DOM) through Arctic hillslopes. DOM export velocities through organic (red arrows) and mineral (blue arrows) soil horizons were not significantly different. However, shifts in vegetation and root exudate deposition, as well as chromatographic fractionation (coiled arrow), influence DOM structural diversity, which increases during downslope export and is greatest along the thawing mineral-permafrost interface.

the residence time of water within the mineral matrix (Angermann et al., 2017; Atchley et al., 2015; Rodhe & Seibert, 2011; Zastruzny et al., 2017). As a result, sustained, lateral dispersion may partially offset rapid export along preferential flow paths in low-gradient catchments and help shape the molecular composition of materials delivered to surface waters (Harms & Jones, 2012; Kawahigashi et al., 2004; Vonk et al., 2015; Ward & Cory, 2015).

DOM composition was strongly related to soil horizon. In pore waters collected from the organic horizon, we observed the highest relative fluorescent intensities of fulvic and humic-type acids. During microbial decomposition, plant-derived molecules are broken into smaller compounds, increasing the relative proportion of polar and ionizable groups (Lehmann & Kleber, 2015). These fragments are more soluble in water and can be preferentially leached from organic to mineral soil horizons (Zhang et al., 2017), where they may accumulate at depth if isolated within the mineral matrix. As a result, the distribution of DOM at depth may be partially independent of preferential flow paths and contribute to incomplete pore water mixing (Neilson et al., 2018). We also observed greater contributions of NMR region I—hydrophobic, aliphatic species primarily related to methylene or methyl-bearing protons—in the organic horizon, and high concentrations of chromophoric DOM (cDOM) at depth, suggesting these exchange mechanisms directly fractionate DOM across the soil profile (Zhang et al., 2017). The soil profile may thus act as a dynamic chromatograph (Kaiser & Kalbitz, 2012), where compounds are selectively retained or leached depending on their solubility, association with the soil mineral matrix, and chemical reactivity (Fellman, Amore, Hood, & Boone, 2008; Lehmann & Kleber, 2015).

The reactivity of OM typically increases with fragmentation and could increase physicochemical complexation with soil minerals (Lehmann & Kleber, 2015), which has been proposed as a mechanism of DOM retention in the Arctic (Schmidt et al., 2011). However, we observed similar DOC concentrations exported through mineral and organic soil horizons, suggesting that large DOM pools are mobile at depth and may be the result of continual DOM sorption and dissolution from the mineral matrix (Kaiser & Kalbitz, 2012). The chemical signature of DOM leaching from surface to deep soil horizons and flowing along the permafrost-interface could reflect sequential and intensive microbial processing during export, leading to a divergence of DOM chemistries in riparian versus hillslope positions (Liang et al., 2017; Wickland et al., 2007; Zhang et al., 2017). Leaching of DOM from rhizosphere organic soils to permafrost-influenced mineral soils may therefore be an important mechanism of OM translocation (Zhang et al., 2017) with the potential to stimulate deep-horizon metabolism (Fontaine et al., 2007).

Pore waters collected at the mineral-permafrost interface had the highest and most variable relative fluorescent intensities of simple aromatic proteins and soluble microbial byproducts (Chen et al., 2003). Although we observed higher $SUVA_{254}$ values at depth, resonance within NMR region IV, associated with aromatic, amide, and phenolic structures (Pautler et al., 2010), was lower in deep mineral than organic soils. Notably, the most abundant metabolites collected at the permafrost-mineral interface were nonchromophoric compounds, including formate and fumarate—carboxylic acids associated with microbial degradation of aromatic compounds—and xanthine, a purine-derived metabolite associated with secondary plant metabolism (Feunang et al., 2016). This observation highlights the need for careful interpretation of EEMS and $SUVA_{254}$ indices, which resolve only cDOM (Spencer et al., 2015; Zhang et al., 2017). We also observed higher ammonium concentrations (and lower C:N ratios) in permafrost-influenced pore waters, suggesting greater microbial turnover of deep OM (Ward & Cory, 2015). Alternatively, physical leaching of N-rich compounds from the organic horizon could increase N availability at depth, amplifying the direct effects of warming on microbial activity (Schmidt et al., 2011). While pore water nitrate concentrations were below detection limit during late-season sampling, autumn concentrations typically range between 0.1 and 1.0 μM (Abbott et al., 2014; Darrouzet-Nardi & Weintraub, 2014; Harms et al., 2016; Harms & Jones, 2012). Release of nitrate at the permafrost thaw front and low rates of denitrification at depth are expected to increase N export from hillslopes to surface waters (Harms & Jones, 2012; Jones et al., 2005; McClelland et al., 2007; Vonk et al., 2015), particularly in catchments experiencing greater hillslope discharge and vertical thaw (Harms & Ludwig, 2016). Regardless of source, our results suggest warming-induced thaw at the permafrost-mineral interface will increase the fraction of cDOM and N-rich products released to the fluvial network.

Landscape characteristics, including topography and topology, are often modeled as first-order controls on runoff characteristics and hillslope-riparian connectivity (Jencso et al., 2010) and appear to control the structural diversity of DOM at our field site. However, the distribution of metabolite diversity ran contrary to our prediction, with higher molecular diversity observed in riparian than hillslope landscape positions. While the structural chemistry in hillslope soils was relatively homogenous, NMR region III and EEMS regions III and V—indicative of plant-derived structures (Chen et al., 2003; Simpson et al., 2003)—were elevated in organic soil horizons. The assimilation of carbohydrates and other labile plant-derived compounds into microbial biomass (Ernakovich et al., 2017; Lynch et al., 2018) could explain the reduced DOM heterogeneity (Liang et al., 2017) we observed in hillslope soils, which are colonized by productive dwarf shrub and tussock-forming sedge communities (Walker & Walker, 1996, Figure 5). Recent evidence suggests widespread shrub expansion (Sturm et al., 2001) will shift rooting distributions (Iversen et al., 2015) and deposition of labile root exudates (Zhu et al., 2016) upward into surface organic horizons that are less vulnerable to priming than energy depleted mineral soils (Fontaine et al., 2007; Wild et al., 2014). If microbial communities utilize new plant inputs with high efficiency (Lynch et al., 2018; Wickland et al., 2007), greater microbial retention and lower OM conversion to CO_2 or CH_4 may increase the abundance of microbe-derived DOM, thereby reducing chemical diversity.

Pore waters collected from riparian soils exhibited higher chemical diversity than those collected from hillslope soils. This downslope divergence in DOM composition could be related to diverse, sequential metabolism during transport (Liang et al., 2017; Mu et al., 2017) or to the accumulation of compounds in a less favorable, or spatially heterogeneous, redox environment. In particular, within riparian pore waters we observed high contributions of soluble microbial-type proteins, determined by fluorescence spectroscopy, and compounds with proton resonance in NMR region II. Detailed NMR and FT-ICR-MS studies of NMR region II in samples collected from marine and freshwater environments revealed a high abundance of carboxyl-rich alicyclic molecules (Hertkorn et al., 2006; Lam et al., 2007). These structures are highly oxidized and enriched in polycarboxylated fused-ring moieties that resist microbial turnover and accumulate in deep ocean DOM pools (Hertkorn et al., 2006). While our pore waters clearly contain compounds in addition to carboxyl-rich alicyclic molecules (Table S4) their presence in the terrestrial environment could link riparian source with oceanic sink and should be verified using targeted, multidimensional NMR experiments (Lam et al., 2007). We also observed a significant decrease in pore water C:N, suggesting DOM pools acquire an increasingly microbial signature during downslope export, independent of soil horizon. Greater DOM diversity in riparian soils could also be due to diverse microbial communities exploiting multiple redox niches (Ernakovich & Wallenstein, 2015; Vos et al., 2013), limited denitrification at depth (Harms & Ludwig, 2016), or selective physicochemical preservation driven by DOM redox reactivity and position within the landscape. Spatial heterogeneity of redox gradients has been linked to the activation of metabolic pathways utilizing alternate terminal electron acceptors to degrade DOM (Boye et al., 2017; Danczak et al., 2016), including siderophores and other chelating agents that are abundant in low-lying Arctic environments (Lipson et al., 2012). We observed relatively high concentrations of metabolites associated with fermentation pathways (including acetate, formate, acetyl phosphate, and methanol) in riparian soils. These metabolites were far less abundant or absent in organic hillslope soils. The combination of variable redox gradients and siderophore availability could contribute to OM metabolism in riparian soils. While highly processed DOM is expected to be a poor energy substrate (Marín-Spiotta et al., 2014), there is evidence that these compounds have high biological and photochemical lability (Abbott et al., 2014; Vonk et al., 2013) in lakes (Woods, Simpson, Pautler, et al., 2011) and rivers (Spencer et al., 2015).

Together, our results suggest that pore water movement through low-gradient, headwater catchments could rapidly mobilize substantial amounts of DOM across the terrestrial-aquatic interface. While the chromatographic influence of surface soils and flow path connectivity will determine the persistence and movement of terrestrial-derived OM across the landscape, the chemical composition of mobilized DOM will structure microbial community composition and metabolism throughout terrestrial and fluvial networks. Our work highlights the need to integrate landscape and spatial characteristics into a framework of C transport in Arctic watersheds.

Acknowledgments
We thank Dr. Ann Hess for statistics consultation, Toolik GIS for assistance collecting spatial data, and two anonymous reviewers, whose thoughtful comments significantly improved our manuscript. This research was supported by a National Science Foundation CAREER award to M. D. W. (255228), a Department of Energy Terrestrial and Ecosystem Science program award to M. D. W. (DE-SC0010568), and a Department of Energy Office of Science Graduate Student Research program award to L. M. L. (DE-SC0014664). Support was also provided by the National Science Foundation Arctic LTER program (1637459). A portion of this research was performed using EMSL, a DOE Office of Science User Facility sponsored by the Office of Biological and Environmental Research and located at Pacific Northwest National Laboratory supported by DOE contract DE-AC05-76RL01830. The authors declare no conflicts of interest. All data and metadata are available through ACADIS, the Advanced Cooperative Arctic Data and Information Service (https://doi.org/10.18739/A2RF5KF5N).

References

Abbott, B. W., Larouche, J. R., Jones, J. B., Bowden, W. B., & Balser, A. W. (2014). Elevated dissolved organic carbon biodegradability from thawing and collapsing permafrost. *Journal of Geophysical Research: Biogeosciences*, *119*, 2049–2063. https://doi.org/10.1002/2014JG002678

Adams, R. W., Holroyd, C. M., Aguilar, J. A., Nilsson, M., & Morris, G. A. (2013). Perfecting WATERGATE: Clean proton NMR spectra from aqueous solution chemical communications, 49(4), 358-360. *Chemical Communications*, *49*(4), 358–360. https://doi.org/10.1002/anie.200

Ameli, A. A., Amvrosiadi, N., Grabs, T., Laudon, H., Creed, I. F., McDonnell, J. J., & Bishop, K. (2016). Hillslope permeability architecture controls on subsurface transit time distribution and flow paths. *Journal of Hydrology*, *543*, 17–30. https://doi.org/10.1016/j.jhydrol.2016.04.071

Anderson, A. E., Weiler, M., Alila, Y., & Hudson, R. O. (2008). Dye staining and excavation of a lateral preferential flow network. *Hydrology and Earth System Sciences Discussions*, *5*(2), 1043–1065. https://doi.org/10.5194/hessd-5-1043-2008

Angermann, L., Jackisch, C., Allroggen, N., Sprenger, M., Zehe, E., Tronicke, J., et al. (2017). Form and function in hillslope hydrology: Characterization of subsurface flow based on response observations. *Hydrology and Earth System Sciences*, *21*(7), 3727–3748. https://doi.org/10.5194/hess-21-3727-2017

Atchley, A. L., Painter, S. L., Harp, D. R., Coon, E. T., Wilson, C. J., Liljedahl, A. K., & Romanovsky, V. E. (2015). Using field observations to inform thermal hydrology models of permafrost dynamics with ATS (v0.83). *Geoscientific Model Development*, *8*(9), 2701–2722. https://doi.org/10.5194/gmd-8-2701-2015

Bates, D., Maechler, M., & Walker, S. (2016). Package "lme4": Linear mixed-effects models. CRAN repository 1–113. https://doi.org/10.18637/jss.v067.i01

Battin, T. J., Kaplan, L. A., Findlay, S., Hopkinson, C. S., Marti, E., Packman, A. I., et al. (2009). Biophysical controls on organic carbon fluxes in fluvial networks. *Nature Geoscience*, *2*(8), 595–595. https://doi.org/10.1038/ngeo602

Battin, T. J., Luyssaert, S., Kaplan, L. A., Aufdenkampe, A. K., Richter, A., & Tranvik, L. J. (2009). The boundless carbon cycle. *Nature Geoscience*, *2*(9), 598–600. https://doi.org/10.1038/ngeo618

Blaen, P. J., Hannah, D. M., Brown, L. E., & Milner, A. M. (2014). Water source dynamics of high Arctic river basins. *Hydrological Processes*, *28*(10), 3521–3538. https://doi.org/10.1002/hyp.9891

Bowden, W. B., Gooseff, M. N., Balser, A., Green, A., Peterson, B. J., & Bradford, J. (2008). Sediment and nutrient delivery from thermokarst features in the foothills of the North Slope, Alaska: Potential impacts on headwater stream ecosystems. *Journal of Geophysical Research*, *113*, G02026. https://doi.org/10.1029/2007JG000470

Boye, K., Noël, V., Tfaily, M. M., Bone, S. E., Williams, K. H., Bargar, J. R., & Fendorf, S. (2017). Thermodynamically controlled preservation of organic carbon in floodplains. *Nature Geoscience*, *10*(6), 415–419. https://doi.org/10.1038/NGEO2940

Carey, S. K., & Quinton, W. L. (2005). Evaluating runoff generation during summer using hydrometric, stable isotope and hydrochemical methods in a discontinuous permafrost alpine catchment. *Hydrological Processes*, *19*, 95–114. https://doi.org/10.1002/hyp.5764

Carey, S. K., & Woo, M. K. (2000). The role of soil pipes as a slope runoff mechanism, subarctic Yukon, Canada. *Journal of Hydrology*, *233*(1-4), 206–222. https://doi.org/10.1016/S0022-1694(00)00234-1

Chen, W., Westerhoff, P., Leenheer, J. A., & Booksh, K. (2003). Fluorescence excitation-emission matrix regional integration to quantify spectra for dissolved organic matter. *Environmental Science and Technology*, *37*(24), 5701–5710. https://doi.org/10.1021/es034354c

Coble, P. G., Lead, J., Baker, A., Reynolds, D. M., & Spencer, R. G. M. (2014). *Aquatic organic matter fluorescence*. Cambridge: Cambridge University Press. https://doi.org/10.1017/CBO9781139045452

Cooper, L. W., Solis, C., Kane, D. L., & Hinzman, L. D. (1993). Application of oxygen-18 tracer techniques to Arctic hydrological processes published by: INSTAAR, University of Colorado Stable URL: http://www.jstor.org/stable/15518. *Arctic and Alpine Research*, *25*(3), 247–255. https://doi.org/10.2307/1551821

Cory, R. M., Crump, B. C., Dobkowski, J. A., & Kling, G. W. (2013). Surface exposure to sunlight stimulates CO_2 release from permafrost soil carbon in the Arctic. *Proceedings of the National Academy of Sciences of the United States of America*, *110*(9), 3429–3434. https://doi.org/10.1073/pnas.1214104110

Cotrufo, M. F., Wallenstein, M. D., Boot, C. M., Denef, K., & Paul, E. (2013). The Microbial Efficiency-Matrix Stabilization (MEMS) framework integrates plant litter decomposition with soil organic matter stabilization: Do labile plant inputs form stable soil organic matter? *Global Change Biology*, *19*(4), 988–995. https://doi.org/10.1111/gcb.12113

Covino, T. (2017). Hydrologic connectivity as a framework for understanding biogeochemical flux through watersheds and along fluvial networks. *Geomorphology*, *277*, 133–144. https://doi.org/10.1016/j.geomorph.2016.09.030

Dalcin Martins, P., Hoyt, D. W., Bansal, S., Mills, C. T., Tfaily, M., Tangen, B. A., et al. (2017). Abundant carbon substrates drive extremely high sulfate reduction rates and methane fluxes in Prairie Pothole Wetlands. *Global Change Biology*, *23*(8), 3107–3120. https://doi.org/10.1111/gcb.13633

Daly, R. A., Borton, M. A., Wilkins, M. J., Hoyt, D. W., Kountz, D. J., Wolfe, R. A., et al. (2016). Microbial metabolisms in a 2.5-km-deep ecosystem created by hydraulic fracturing in shales. *Nature Microbiology*, *1*(10), 1–9. https://doi.org/10.1038/nmicrobiol.2016.146

Danczak, R. E., Sawyer, A. H., Williams, K. H., Stegen, J. C., Hobson, C., & Wilkins, M. J. (2016). Seasonal hyporheic dynamics control coupled microbiology and geochemistry in Colorado River sediments. *Journal of Geophysical Research: Biogeosciences*, *121*, 2976–2987. https://doi.org/10.1002/2016JG003527

Darrouzet-Nardi, A., & Weintraub, M. N. (2014). Evidence for spatially inaccessible labile N from a comparison of soil core extractions and soil pore water lysimetry. *Soil Biology and Biochemistry*, *73*, 22–32. https://doi.org/10.1016/j.soilbio.2014.02.010

Davis, S. N., Thompson, G. M., Bentley, H. W., & Stiles, G. (1980). Ground-water tracers—A short review. *Groundwater*, *18*(1), 14–23. https://doi.org/10.1111/j.1745-6584.1980.tb03366.x

Duffy, J. E., Lefcheck, J. S., Stuart-Smith, R. D., Navarrete, S. A., & Edgar, G. J. (2016). Biodiversity enhances reef fish biomass and resistance to climate change. *Proceedings of the National Academy of Sciences*, *113*(22), 6230–6235. https://doi.org/10.1073/pnas.1524465113

Ernakovich, J. G., Lynch, L. M., Brewer, P. E., Calderon, F. J., & Wallenstein, M. D. (2017). Redox and temperature-sensitive changes in microbial communities and soil chemistry dictate greenhouse gas loss from thawed permafrost. *Biogeochemistry*, *134*(1-2), 183–200. https://doi.org/10.1007/s10533-017-0354-5

Ernakovich, J. G., & Wallenstein, M. D. (2015). Permafrost microbial community traits and functional diversity indicate low activity at in situ thaw temperatures. *Soil Biology and Biochemistry*, *87*, 78–89. https://doi.org/10.1016/j.soilbio.2015.04.009

Fellman, J.B., D'Amore, D.V., Hood, E., & Boone, R.D. (2008). Fluorescence characteristics and biodegradability of dissolved organic matter in forest and wetland soils from coastal temperate watersheds in Southeast Alaska. *Biogeochemistry 88*, 169–184. https://doi.org/10.1007/s10533-008-9203-x

Fellman, J. B., D'Amore, D. V., & Hood, E. (2008). An evaluation of freezing as a preservation technique for analyzing dissolved organic C, N and P in surface water samples. *Science of the Total Environment*, *392*(2-3), 305–312. https://doi.org/10.1016/j.scitotenv.2007.11.027

Feunang, Y. D., Eisner, R., Knox, C., Chepelev, L., Hastings, J., Owen, G., et al. (2016). ClassyFire: Automated chemical classification with a comprehensive, computable taxonomy. *Journal of Cheminformatics*, *8*(1), 61–20. https://doi.org/10.1186/s13321-016-0174-y

Fontaine, S., Barot, S., Barré, P., Bdioui, N., Mary, B., & Rumpel, C. (2007). Stability of organic carbon in deep soil layers controlled by fresh carbon supply. *Nature*, *450*(7167), 277–280. https://doi.org/10.1038/nature06275

Fox, J., & Monette, G. (1992). Generalized collinearity diagnostics. *Journal of the American Statistical Association*, *87*(417), 178–183. https://doi.org/10.1080/01621459.1992.10475190

Frey, K. E., & McClelland, J. W. (2009). Impacts of permafrost degradation on arctic river biogeochemistry. *Hydrological Processes*, *23*(1), 169–182. https://doi.org/10.1002/hyp

Giesy, J. P., & Briese, L. A. (1978). Particulate formation due to freezing humic waters. *Water Resources Research*, *14*(3), 542–544. https://doi.org/10.1029/WR014i003p00542

Grootveld, M. (2014). Introduction to the applications of chemometric techniques in omics research: Common pitfalls, misconceptions and rights and wrongs. In *Metabolic profiling: Disease and xenobiotics* (Chap. 1, pp. 1–34). Cambridge. https://doi.org/10.1039/9781849735162-00001

Hackstadt, A. J., & Hess, A. M. (2009). Filtering for increased power for microarray data analysis. *BMC Bioinformatics*, *10*(1), 11. https://doi.org/10.1186/1471-2105-10-11

Harms, T. K., Edmonds, J. W., Genet, H., Creed, I. F., Aldred, D., Balser, A., & Jones, J. B. (2016). Catchment influence on nitrate and dissolved organic matter in Alaskan streams across a latitudinal gradient. *Journal of Geophysical Research: Biogeosciences*, *121*, 350–369. https://doi.org/10.1002/2015JG003201

Harms, T. K., & Jones, J. B. (2012). Thaw depth determines reaction and transport of inorganic nitrogen in valley bottom permafrost soils. *Global Change Biology*, *18*(9), 2958–2968. https://doi.org/10.1111/j.1365-2486.2012.02731.x

Harms, T. K., & Ludwig, S. M. (2016). Retention and removal of nitrogen and phosphorus in saturated soils of arctic hillslopes. *Biogeochemistry*, *127*(2-3), 291–304. https://doi.org/10.1007/s10533-016-0181-0

Herndon, E., AlBashaireh, A., Singer, D., Roy Chowdhury, T., Gu, B., & Graham, D. (2017). Influence of iron redox cycling on organo-mineral associations in Arctic tundra soil. *Geochimica et Cosmochimica Acta*, *207*, 210–231. https://doi.org/10.1016/j.gca.2017.02.034

Hertkorn, N., Benner, R., Frommberger, M., Schmitt-Kopplin, P., Witt, M., Kaiser, K., et al. (2006). Characterization of a major refractory component of marine dissolved organic matter. *Geochimica et Cosmochimica Acta*, *70*(12), 2990–3010. https://doi.org/10.1016/j.gca.2006.03.021

Hinton, M. J., Schiff, S. L., & English, M. C. (1994). Examining the contributions of glacial till water to storm runoff using two- and three-component hydrograph separations. *Water Resources Research*, *30*(4), 983–993. https://doi.org/10.1029/93WR03246

Iversen, C. M., Sloan, V. L., Sullivan, P. F., Euskirchen, E. S., Mcguire, A. D., Norby, R. J., et al. (2015). The unseen iceberg: Plant roots in arctic tundra. *New Phytologist*, *205*(1), 34–58. https://doi.org/10.1111/nph.13003

Jansen, B., Kalbitz, K., & McDowell, W. H. (2014). Dissolved organic matter: Linking soils and aquatic systems. *Vadose Zone Journal*, *13*(7), 0. https://doi.org/10.2136/vzj2014.05.0051

Jencso, K. G., McGlynn, B. L., Gooseff, M. N., Bencala, K. E., & Wondzell, S. M. (2010). Hillslope hydrologic connectivity controls riparian groundwater turnover: Implications of catchment structure for riparian buffering and stream water sources. *Water Resources Research*, *46*, W10524. https://doi.org/10.1029/2009WR008818

Jenness, J. S. (2004). Calculating landscape surface area from digital elevation models. *Wildlife Society Bulletin*, *32*(3), 829–839. https://doi.org/10.2193/0091-7648(2004)032[0829:CLSAFD]2.0.CO;2

Jones, J. B., Petrone, K. C., Finlay, J. C., Hinzman, L. D., & Bolton, W. R. (2005). Nitrogen loss from watersheds of interior Alaska underlain with discontinuous permafrost. *Geophysical Research Letters*, *32*, L02401. https://doi.org/10.1029/2004GL021734

Kaiser, K., & Kalbitz, K. (2012). Cycling downwards - dissolved organic matter in soils. *Soil Biology and Biochemistry*, *52*, 29–32. https://doi.org/10.1016/j.soilbio.2012.04.002

Kalbitz, K., Schwesig, D., Schmerwitz, J., Kaiser, K., Haumaier, L., Glaser, B., et al. (2003). Changes in properties of soil-derived dissolved organic matter induced by biodegradation. *Soil Biology and Biochemistry*, *35*(8), 1129–1142. https://doi.org/10.1016/S0038-0717(03)00165-2

Kane, D. L., Hinzman, L. D., Benson, C. S., & Everett, K. R. (1989). Hydrology of Imnavait Creek, an arctic watershed. *Ecography*, *12*(3), 262–269. https://doi.org/10.1111/j.1600-0587.1989.tb00845.x

Kawahigashi, M., Kaiser, K., Kalbitz, K., Rodionov, A., & Guggenberger, G. (2004). Dissolved organic matter in small streams along a gradient from discontinuous to continuous permafrost. *Global Change Biology*, *10*(9), 1576–1586. https://doi.org/10.1111/j.1365-2486.2004.00827.x

Keiluweit, M., Bougoure, J. J., Nico, P. S., Pett-Ridge, J., Weber, P. K., & Kleber, M. (2015). Mineral protection of soil carbon counteracted by root exudates. *Nature Climate Change*, *5*(6), 588–595. https://doi.org/10.1038/nclimate2580

Keiluweit, M., Wanzek, T., Kleber, M., Nico, P., & Fendorf, S. (2017). Anaerobic microsites have an unaccounted role in soil carbon stabilization. *Nature Communications*, *8*(1), 1771–1710. https://doi.org/10.1038/s41467-017-01406-6

Kellerman, A. M., Dittmar, T., Kothawala, D. N., & Tranvik, L. J. (2014). Chemodiversity of dissolved organic matter in lakes driven by climate and hydrology. *Nature Communications*, *5*(1), 1–8. https://doi.org/10.1038/ncomms4804

Kirchner, J. W. (2003). A double paradox in catchment hydrology and geochemistry. *Hydrological Processes*, *17*, 871–874. Invited Commentary. https://doi.org/10.1002/hyp.5108

Klaus, J., Zehe, E., Elsner, M., Külls, C., & McDonnell, J. J. (2013). Macropore flow of old water revisited: Experimental insights from a tile-drained hillslope. *Hydrology and Earth System Sciences*, *17*(1), 103–118. https://doi.org/10.5194/hess-17-103-2013

Kling, G. W. (2007). *Imnavait watershed thaw depth survey summary for 2003 to present, Arctic LTER, Toolik Research Station*. Environmental Data Initiative: Alaska.

Koch, J. C., Runkel, R. L., Striegl, R., & Mcknight, D. M. (2013). Hydrologic controls on the transport and cycling of carbon and nitrogen in a boreal catchment underlain by continuous permafrost. *Journal of Geophysical Research: Biogeosciences*, *118*, 698–712. https://doi.org/10.1002/jgrg.20058

Koven, C., Friedlingstein, P., Ciais, P., Khvorostyanov, D., Krinner, G., & Tarnocai, C. (2009). On the formation of high-latitude soil carbon stocks: Effects of cryoturbation and insulation by organic matter in a land surface model. *Geophysical Research Letters*, *36*, L21501. https://doi.org/10.1029/2009GL040150

Lachenbruch, A. H. (1962). Mechanics of thermal contraction cracks and ice-wedge polygons in permafrost. *Geological Society of America Special Papers*, *70*, 1–66. https://doi.org/10.1130/SPE70-p1

Lam, B., Baer, A., Alaee, M., Lefebvre, B., Moser, A., Williams, A., & Simpson, A. J. (2007). Major structural components in freshwater dissolved organic matter. *Environmental Science & Technology*, *41*(24), 8240–8247. https://doi.org/10.1021/es0713072

Lehmann, J., Kleber, M., 2015. The contentious nature of soil organic matter. Perspective. *Nature 528*, 60–68. https://doi.org/10.1038/nature16069

Lenth, R., (2016). Package lsmeans: Least-squares means. CRAN repository.

Liang, C., Schimel, J. P., & Jastrow, J. D. (2017). The importance of anabolism in microbial control over soil carbon storage. *Nature Microbiology*, *2*(8), 17105. https://doi.org/10.1038/nmicrobiol.2017.105

Lipson, D. A., Zona, D., Raab, T., Bozzolo, F., Mauritz, M., & Oechel, W. (2012). Water-table height and microtopography control biogeochemical cycling in an Arctic coastal tundra ecosystem. *Biogeosciences*, *9*(1), 577–591. https://doi.org/10.5194/bg-9-577-2012

Lynch, L. M., Machmuller, M. B., Cotrufo, M. F., Paul, E. A., & Wallenstein, M. D. (2018). Tracking the fate of fresh carbon in the Arctic tundra: Will shrub expansion alter responses of soil organic matter to warming? *Soil Biology & Biochemistry*, *120*, 134–144. https://doi.org/10.1016/j.soilbio.2018.02.002

Marín-Spiotta, E., Gruley, K. E., Crawford, J., Atkinson, E. E., Miesel, J. R., Greene, S., et al. (2014). Paradigm shifts in soil organic matter research affect interpretations of aquatic carbon cycling: Transcending disciplinary and ecosystem boundaries. *Biogeochemistry*, *117*(2-3), 279–297. https://doi.org/10.1007/s10533-013-9949-7

McCay, R. T. (2009). Recent advances in solvent suppression for solution NMR: A practical reference. In G. A. Webb (Ed.), *Annual reports on NMR spectroscopy* (pp. 33–76). San Diego, CA: Academic Press.

McClelland, J. W., Stieglitz, M., Pan, F., Holmes, R. M., & Peterson, B. J. (2007). Recent changes in nitrate and dissolved organic carbon export from the upper Kuparuk River, North Slope, Alaska. *Journal of Geophysical Research*, *112*, G04S60. https://doi.org/10.1029/2006JG000371

McNamara, J. P., Kane, D. L., Hobbie, J. E., & Kling, G. W. (2008). Hydrologic and biogeochemical controls on the spatial and temporal patterns of nitrogen and phosphorus in the Kuparuk River, Arctic Alaska. *Hydrological Processes*, *22*(17), 3294–3309. https://doi.org/10.1002/hyp

Mu, C. C., Abbott, B. W., Wu, X. D., Zhao, Q., Wang, H. J., Su, H., et al. (2017). Thaw depth determines dissolved organic carbon concentration and biodegradability on the northern Qinghai-Tibetan plateau. *Geophysical Research Letters*, *44*, 9389–9399. https://doi.org/10.1002/2017GL075067

Natali, S. M., Schuur, E. A. G., Mauritz, M., Schade, J. D., Celis, G., Crummer, K. G., et al. (2015). Permafrost thaw and soil moisture driving CO_2 and CH_4 release from upland tundra. *Journal of Geophysical Research: Biogeosciences.*, *120*, 525–537. https://doi.org/10.1002/2014JG002872

Natali, S. M., Schuur, E. A. G., & Rubin, R. L. (2012). Increased plant productivity in Alaskan tundra as a result of experimental warming of soil and permafrost. *Journal of Ecology*, *100*(2), 488–498. https://doi.org/10.1111/j.1365-2745.2011.01925.x

Neilson, B. T., Cardenas, M. B., O'Connor, M. T., Rasmussen, M. T., King, T. V., & Kling, G. W. (2018). Groundwater flow and exchange across the land surface explain carbon export patterns in continuous permafrost watersheds. *Geophysical Research Letters*, *45*, 7596–7605. https://doi.org/10.1029/2018GL078140

Oksanen, J., Kindt, R., Legendre, P., O'Hara, B., Stevens, H.H., (2007). The vegan package.

Osterkamp, T. E., & Romanovsky, V. E. (1999). Evidence for warming and thawing of discontinuous permafrost in Alaska. *Permafrost and Periglacial Processes*, *10*(1), 17–37. https://doi.org/10.1002/(SICI)1099-1530(199901/03)10:1<17::AID-PPP303>3.0.CO;2-4

Otero, M., Mendonça, A., Válega, M., Santos, E. B. H., Pereira, E., Esteves, V. I., & Duarte, A. (2007). Fluorescence and DOC contents of estuarine pore waters from colonized and non-colonized sediments: Effects of sampling preservation. *Chemosphere*, *67*(2), 211–220. https://doi.org/10.1016/j.chemosphere.2006.10.044

Pautler, B. G., Simpson, J., Mcnally, D. J., & Lamoureux, S. F. (2010). Arctic permafrost active layer detachments stimulate microbial activity and degradation of soil organic matter. *Environmental Science and Technology*, *44*(11), 4076–4082. https://doi.org/10.1021/es903685j

Pokrovsky, O. S., Karlsson, J., & Giesler, R. (2018). Freeze-thaw cycles of Arctic thaw ponds remove colloidal metals and generate low-molecular-weight organic matter. *Biogeochemistry*, *137*(3), 321–336. https://doi.org/10.1007/s10533-018-0421-6

Riseborough, D., Shiklomanov, N., Etzelmuller, B., Gruber, S., & Marchenko, S. (2008). Recent advances in permafrost modeling. *Permafrost and Periglacial Processes*, *19*(2), 137–156. https://doi.org/10.1002/ppp

Rist, M. J., Muhle-Goll, C., Görling, B., Bub, A., Heissler, S., Watzl, B., & Luy, B. (2013). Influence of freezing and storage procedure on human urine samples in NMR-based metabolomics. *Metabolites*, *3*(2), 243–258. https://doi.org/10.3390/metabo3020243

Rodhe, A., & Seibert, J. (2011). Groundwater dynamics in a till hillslope: Flow directions, gradients and delay. *Hydrological Processes*, *25*(12), 1899–1909. https://doi.org/10.1002/hyp.7946

Roth, V.-N., Dittmar, T., Gaupp, R., & Gleixner, G. (2014). Ecosystem-specific composition of dissolved organic matter. *Vadose Zone Journal*, 13.

Rowland, J., Jones, C., Altman, G., Bryan, R., Crosby, B., Hinzman, L. D., et al. (2010). Arctic landscapes in transition: Responses to thawing permafrost Arctic landscapes in transition: Responses to thawing permafrost. *Eos*, *91*(26), 229–230. https://doi.org/10.1029/2010EO260001

Rustad, L. E., Campbell, J. L., Marion, G. M., Norby, R. J., Mitchell, M. J., Hartley, A. E., et al. (2001). A meta-analysis of the response of soil respiration, net nitrogen mineralization, and aboveground plant growth to experimental ecosystem warming. *Oecologia*, *126*(4), 543–562. https://doi.org/10.1007/s004420000544

Santeford, H. S. (1978). Snow soil interactions in interior Alaska. In S. C. Colbeck & R. M. Ray (Eds.), *Modeling of snow cover runoff* (pp. 311–318). Hanover: U. S. Army Cold Regions Research and Engineering Laboratory.

Schmidt, M. W. I., Torn, M. S., Abiven, S., Dittmar, T., Guggenberger, G., Janssens, I. A., et al. (2011). Persistence of soil organic matter as an ecosystem property. *Nature*, *478*(7367), 49–56. https://doi.org/10.1038/nature10386

Schuur, E. A. G., Vogel, J. G., Crummer, K. G., Lee, H., Sickman, J. O., & Osterkamp, T. E. (2009). The effect of permafrost thaw on old carbon release and net carbon exchange from tundra. *Nature*, *459*(7246), 556–559. https://doi.org/10.1038/nature08031

Seibert, J., Grabs, T., Köhler, S., Laudon, H., Winterdahl, M., & Bishop, K. (2009). Linking soil-and stream-water chemistry based on a riparian flow-concentration integration model. *Hydrology and Earth System Sciences*, *6*(4), 5603–5629. https://doi.org/10.5194/hessd-6-5603-2009

Simpson, A. J., Kingery, W. L., & Hatcher, P. G. (2003). The identification of plant derived structures in humic materials using three-dimensional NMR spectroscopy. *Environmental Science and Technology*, *37*(2), 337–342. https://doi.org/10.1021/es025956j

Simpson, A. J., Simpson, M. J., Smith, E., & Kelleher, B. P. (2007). Microbially derived inputs to soil organic matter: Are current estimates too low? *Environmental Science and Technology*, *41*(23), 8070–8076. https://doi.org/10.1021/es071217x

Simpson, A. J., Simpson, M. J., & Soong, R. (2012). Nuclear magnetic resonance spectroscopy and its key role in environmental research. *Environmental Science and Technology*, *46*(21), 11,488–11,496. https://doi.org/10.1021/es302154w

Spencer, R. G., Hernes, P. J., Ruf, R., Baker, A., Dyda, R. Y., Stubbins, A., & Six, J. (2010). Temporal controls on dissolved organic matter and lignin biogeochemistry in a pristine tropical river, Democratic Republic of Congo. *Journal of Geophysical Research*, *115*, G03013. https://doi.org/10.1029/2009JG001180

Spencer, R. G. M., Mann, P. J., Dittmar, T., Eglinton, T. I., Mcintyre, C., Holmes, R. M., et al. (2015). Detecting the signature of permafrost thaw in Arctic rivers. *Geophysical Research Letters*, *42*, 2830–2835. https://doi.org/10.1002/2015GL063498

Sturm, M., Racine, C., & Tape, K. (2001). Climate change. Increasing shrub abundance in the Arctic. *Nature*, *411*(6837), 546–547. https://doi.org/10.1038/35079180

Sutfin, N. A., & Wohl, E. (2017). Substantial soil organic carbon retention along floodplains of mountain streams. *Journal of Geophysical Research: Earth Surface*, *122*, 1325–1338. https://doi.org/10.1002/2016JF004004

Tetzlaff, D., Buttle, J., Carey, S. K., Mcguire, K., Laudon, H., & Soulsby, C. (2015). Tracer-based assessment of flow paths, storage and runoff generation in northern catchments: A review. *Hydrological Processes*, *29*(16), 3475–3490. https://doi.org/10.1002/hyp.10412

Vierling, L. A., Eitel, J. U. H., Boelman, N. T., Griffin, K. L., Greaves, H., Magney, T. S., et al. (2013). Bare earth LiDaR dataset for Toolik Field Station, AK, and nearby field sites along Dalton Highway.

Vonk, J. E., Mann, P. J., Davydov, S., Davydova, A., Spencer, R. G. M., Schade, J. D., et al. (2013). High biolability of ancient permafrost carbon upon thaw. *Geophysical Research Letters*, *40*, 2689–2693. https://doi.org/10.1002/grl.50348

Vonk, J. E., Tank, S. E., Bowden, W. B., Laurion, I., Vincent, W. F., Alekseychik, P., et al. (2015). Reviews and syntheses: Effects of permafrost thaw on Arctic aquatic. *Biogeosciences*, *12*(23), 7129–7167. https://doi.org/10.5194/bg-12-7129-2015

Vos, M., Wolf, A., Jennings, S., & Kowalchuk, G. (2013). Micro-scale determinants of bacterial diversity in soil. *FEMS Microbiology Reviews*, *37*(6), 936–954. https://doi.org/10.1111/1574-6976.12023

Waldrop, M. P., Wickland, K. P., White Iii, R., Berhe, A. A., Harden, J. W., & Romanovsky, V. E. (2010). Molecular investigations into a globally important carbon pool: Permafrost-protected carbon in Alaskan soils. *Global Change Biology*, *16*, 2543–2554. https://doi.org/10.1111/j.1365-2486.2009.02141.x

Walker, D. A., & Walker, M. D. (1996). Terrain and vegetation of the Imnavait Creek watershed. In *Landscape function and disturbance in Arctic Tundra* (pp. 73–108). Berlin Heidelberg: Springer. https://doi.org/10.1007/978-3-662-01145-4_4

Walvoord, M. A., & Kurylyk, B. L. (2016). Hydrologic impacts of thawing permafrost—A review. *Vadose Zone Journal*, *15*(6), 0. https://doi.org/10.2136/vzj2016.01.0010

Ward, C. P., & Cory, R. M. (2015). Chemical composition of dissolved organic matter draining permafrost soils. *Geochimica et Cosmochimica Acta*, *167*, 63–79. https://doi.org/10.1016/j.gca.2015.07.001

Ward, C. P., Nalven, S. G., Crump, B. C., Kling, G. W., & Cory, R. M. (2017). Photochemical alteration of organic carbon draining permafrost soils shifts microbial metabolic pathways and stimulates respiration. *Nature Communications*, *8*(1), 772–777. https://doi.org/10.1038/s41467-017-00759-2

Wehrens, R., Mevik, B.-H., 2007. pls: Partial least squares regression (PLSR) and principal component regression (PCR). R Package Version 2.1–0.

Weiler, M., & McDonnell, J. J. (2006). Testing nutrient flushing hypotheses at the hillslope scale: A virtual experiment approach. *Journal of Hydrology*, *319*(1-4), 339–356. https://doi.org/10.1016/j.jhydrol.2005.06.040

Weishaar, J., Aiken, G., Bergamaschi, B., Fram, M., Fujii, R., & Mopper, K. (2003). Evaluation of specific ultra-violet absorbance as an indicator of the chemical content of dissolved organic carbon. *Environmental Science and Technology*, *37*(20), 4702–4708. https://doi.org/10.1021/es030360x

White, D., Hinzman, L., Alessa, L., Cassano, J., Chambers, M., Falkner, K., et al. (2007). The arctic freshwater system: Changes and impacts. *Journal of Geophysical Research*, *112*, G04S54. https://doi.org/10.1029/2006JGO00353

Wickland, K. P., Neff, J. C., & Aiken, G. R. (2007). Dissolved organic carbon in Alaskan boreal forest: Sources, chemical characteristics, and biodegradability. *Ecosystems*, *10*(8), 1323–1340. https://doi.org/10.1007/s10021-007-9101-4

Wild, B., Schnecker, J., Alves, R. J. E., Barsukov, P., Barta, J., Capek, P., et al. (2014). Input of easily available organic C and N stimulates microbial decomposition of soil organic matter in arctic permafrost soil. *Soil Biology and Biochemistry*, *75*(100), 143–151. https://doi.org/10.1016/j.soilbio.2014.04.014

Woo, M. (2012). *Permafrost hydrology*. Berlin: Spring Science & Business Media. https://doi.org/10.1007/978-3-642-23462-0

Woods, G. C., Simpson, M. J., Kelleher, B. P., McCaul, M., Kingery, W. L., & Simpson, A. J. (2009). Online high-performance size exclusion chromatography—Nuclear magnetic resonance for the characterization of dissolved organic matter. *Environmental Science and Technology*, *44*, 624–630.

Woods, G. C., Simpson, M. J., Koerner, P. J., Napoli, A., & Simpson, A. J. (2011). HILIC-NMR: Toward the identification of individual molecular components in dissolved organic matter. *Environmental Science & Technology*, *45*(9), 3880–3886. https://doi.org/10.1021/es103425s

Woods, G. C., Simpson, M. J., Pautler, B. G., Lamoureux, S. F., Lafrenière, M. J., & Simpson, A. J. (2011). Evidence for the enhanced lability of dissolved organic matter following permafrost slope disturbance in the Canadian High Arctic. *Geochimica et Cosmochimica Acta*, *75*(22), 7226–7241. https://doi.org/10.1016/j.gca.2011.08.013

Xia, J., & Wishart, D. S. (2016). Using MetaboAnalyst 3.0 for comprehensive metabolomics data analysis. *Current Protocols in Bioinformatics*, *55*, 10.1–14.10.91.

Zastruzny, S. F., Elberling, B., Nielsen, L., & Jensen, K. H. (2017). Water flow in the active layer along an arctic slope—An investigation based on a field campaign and model simulations. *The Cryosphere Discussion*, 1–32.

Zhang, X., Hutchings, J. A., Bianchi, T. S., Liu, Y., Arellano, A. R., & Schuur, E. A. G. (2017). Importance of lateral flux and its percolation depth on organic carbon export in Arctic tundra soil: Implications from a soil leaching experiment. *Journal of Geophysical Research: Biogeosciences*, *122*, 796–810. https://doi.org/10.1002/2016JG003754

Zhu, Q., Riley, W. J., & Tang, J. (2016). A new theory of plant-microbe nutrient competition resolves inconsistencies between observations and model predictions. *Ecological Applications* https://doi.org/10.1002/eap.1490, *27*(3), 875–886.

Zuur, A. F., Ieno, E. N., & Elphick, C. S. (2010). A protocol for data exploration to avoid common statistical problems. *Methods in Ecology and Evolution*, *1*(1), 3–14. https://doi.org/10.1111/j.2041-210X.2009.00001.x